INFLUENCE OF FREE CONVECTION ON THE HEAT TRANSFER CHARACTERISTICS OF DEVELOPING AND FULLY DEVELOPED FLOW IN THE TRANSITIONAL FLOW REGIME

Everts, M. and Meyer J.P.*
*Author for correspondence
Department of Mechanical and Aeronautical Engineering,
University of Pretoria,
Pretoria, 0002,
South Africa,
E-mail: josua.meyer@up.ac.za

ABSTRACT

The transitional flow regime has been mostly avoided by designers due to uncertainty and perceived chaotic behavior. Previous work done in the transitional flow regime did not focus specifically on the effects of free convection on the local heat transfer characteristics along the tube length. Therefore, the purpose of this study was to investigate the effects of free convection on the heat transfer characteristics of developing and fully developed flow in the transitional flow regime; and is work in progress. An experimental set-up was designed, built and validated and heat transfer measurements were taken at a heat fluxes of 1, 3 and 8 kW/m^2 between Reynolds numbers of 100 and 8 000. The Nusselt numbers varied between 4.3 and 80, the Prandtl number between 2.9 and 6.5, the Grashof number between 6.8 and 1.06x10^4 and the Rayleigh number between 43.8 and 3.07x10^4. It was found that the width of the transitional flow regime decreased along the tube length as the flow approached fully developed flow. As the free convection effects were increased by increasing the heat flux, the width of the transitional flow regime decreased further.

INTRODUCTION

Heat exchangers have a wide range of industrial and domestic applications, for example boilers in power plants and air-conditioners in cars and buildings. To ensure efficiency, engineers need accurate correlations to optimise the design of these heat exchangers. As pressure drop is related to pumping power and thus operational running cost, the aim is to obtain high heat transfer coefficients and low pressure drops. In the design process, they usually have a choice to select between a flow regime that is either laminar (low heat transfer coefficients and pressure drops) or turbulent (high heat transfer coefficients and pressure drops). However, the best compromise between high heat transfer coefficients and low pressure drops might be in the transitional flow regime, between laminar and turbulent flow. Furthermore, design constraints, changes in operating conditions or equipment, corrosion and scaling, can also cause that the heat exchangers start to operate in or close to the transitional flow regime. In this flow regime, the flow alternates between laminar and turbulent and turbulent eddies occur in flashes, known as turbulent bursts. This might cause the pressure drop to increase and order of magnitude [1]. Designers are thus usually advised to avoid this flow regime since the flow is believed to be unstable and chaotic, and little design information is available.

Flow regimes have been extensively investigated from as early as 1883, especially focussing on laminar and turbulent flow, while research has been devoted to transitional flow since the 1990s.

NOMENCLATURE

A	[m^2]	Area
cp	[J/kg.K]	Specific heat at constant pressure
D	[m]	Inner diameter
Do	[m]	Outer diameyer
EB	[-]	Energy balance
Gr	[-]	Grashof number
h	[W/m^{2}K]	Heat transfer coefficient
I	[A]	Current
j	[-]	Colburn j-factor
k	[W/mK]	Thermal conductivity
L	[m]	Length
$\dot{m}$	[kg/s]	Mass flow rate
Nu	[-]	Nusselt number
Pr	[-]	Prandtl number
$\dot{Q}$	[W]	Heat transfer rate
$\dot{q}$	[W/m^2]	Heat flux
R	[°C/m]	Thermal resistance
Ra	[-]	Rayleigh number
Re	[-]	Reynolds number
T	[°C]	Temperature
V	[V]	Voltage
x	[m]	Distance from inlet

Special characters

ρ	[kg/m^3]	Density
μ	[kg/m.s]	Dynamic viscosity
ν	[m^2/s]	Kinematic viscosity

Subscripts

b	Bulk
c	Cross-section
cr	Critical Reynolds number
i	Inlet
lre	Low-Reynolds-number-end
m	Mean
o	Outlet/ outer
s	Surface
t	Turbulent

According to a recent review paper by Meyer [1], the transitional flow regime has been mainly investigated by Professor Ghajar from Oklahoma State University and his co-workers and Professor Meyer from the University of Pretoria and his co-workers. Ghajar and co-workers used local temperature and pressure measurements along a tube length to investigate the effect of different inlet geometries and heating on the heat transfer coefficients and friction factors [2-11] A constant heat flux boundary condition and different mixtures of distilled water and ethylene glycol were used, which resulted in very high Prandtl numbers (up to 160). Furthermore, due to the combined effects of the relatively large tube diameter (15.8 mm), and high Prandtl numbers, the Rayleigh numbers were in the order of 10^5 to 10^6 [5]. The Rayleigh number plays an important role in mixed convection heat transfer and is not only used in their flow regime map (to determine whether the flow is dominated by forced or mixed convection) [5], but also in their correlations to predict the Nusselt numbers in the laminar and transitional flow regimes [4].

Meyer and co-workers used a constant surface temperature boundary condition and water as the test fluid, which resulted in significantly lower Prandtl numbers (approximately 7). Furthermore, the fluid was being cooled and not heated. As they considered the average measurements across a tube length, their data contained both developing (laminar and transitional flow regimes) and fully developed (turbulent flow regime) data [12-15]. From literature it is clear that Ghajar and co-workers broke the ground with investigating the effect of inlet geometry and heating on transition, making it possible for others, such as Meyer and co-workers, to follow. However, the focus of previous studies was not on the characteristics of developing flow, but rather on the effect of different inlet geometries and enhanced tubes. Up to now, no experimental studies have been specifically devoted to the heat transfer characteristics of developing flow in the transitional flow regime, how it changes along the tube length, how it differs from that of fully developed flow, as well as the effects of free convection. Therefore, in order to gain a better understanding of the characteristics of developing flow, the purpose of this study was to experimentally investigate the influence of free convection on the heat transfer characteristics of developing and fully developed flow of low Prandtl number fluids in a smooth horizontal tube with a small diameter.

EXPERIMENTAL SET-UP

The experimental set-up is shown in Figure 1 and consisted of a closed water loop which circulated the test fluid from a storage tank through a test section and back using an electronically controlled magnetic gear pump. Water was used as the test fluid and the temperature of the storage tank was kept at 20 ºC using a thermostat bath. As the lab was climate controlled (24/7) to a constant temperature of 21.8 ºC, it was possible to conduct experiments at the same ambient conditions throughout the year.

A pressure relief valve was installed to allow the water to flow directly to the storage tank if the pressure exceeded the preselected threshold. A bypass valve was inserted between the pump and the calming section and also allowed the water to flow back into the tank. The bypass valve was also used to increase the pump speed for a specific flow rate, since the pulsations decreased with increasing pump speed. The valve positions were continually adjusted to minimise the flow pulsations for all the measurements, since the stability of flow is crucial when studying transitional flow.

A calming section, similar to the one used by Ghajar [2-10, 16, 17] was installed prior to the test section to straighten the flow. A Pt100 which was used to measure the inlet water temperature was also housed inside the calming section. A mixing section was installed after the test section to obtain a uniform bulk outlet temperature.

A Coriolis mass flow meter with a capacity of 108 *l*/h and accuracy of 0.05%, was installed after the mixing section to measure the mass flow rates. The mass flow meters had an accuracy of 0.05% and were used according to the flow rate requirements, in order to minimise the uncertainty of the mass flow measurements.

The mass flow rates were controlled by frequency drives that were connected to the pumps, therefore the required flow rate was obtained by increasing or decreasing the pump speed. The frequency drives were also connected to a personal computer via a data acquisition system. A Labview program was used to record the data points and a MATLAB program was used to read the measured raw data and process the results.

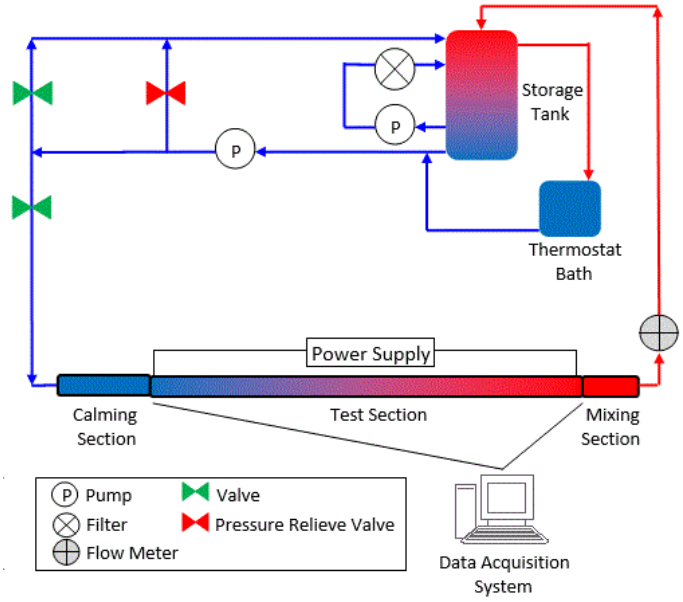

Figure 1 Schematic of experimental set-up used to conduct heat transfer measurements.

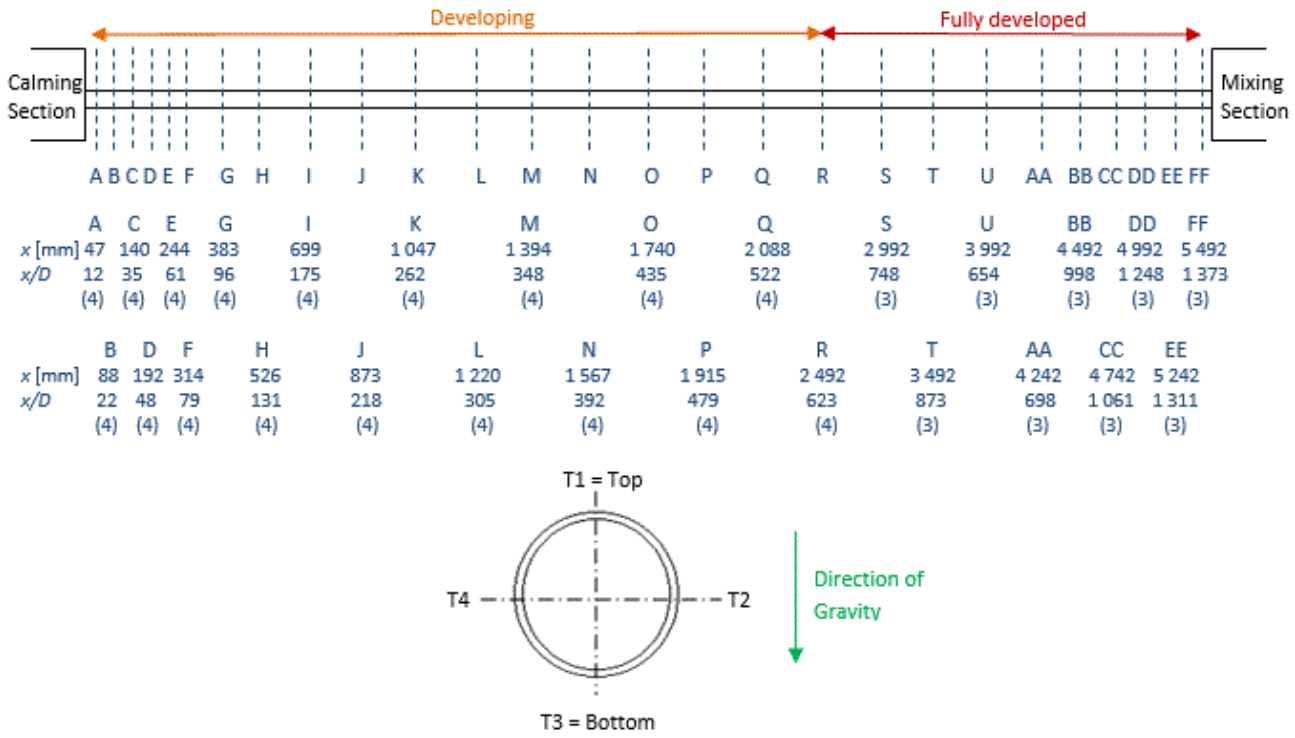

Figure 2 Schematic representation of the test section indicating 18 developing flow thermocouple stations, A-R, and 9 fully developed flow thermocouple stations. A cross-sectional view of the test section is also included to indicate the four thermocouples (T1 to T4) spaced around the periphery of the tube. Stations A-R contained 4 thermocouples each (T1 to T4), while stations S-FF contained three thermocouples each (T1, T3 and alternating T2 and T4)

A square-edged inlet was used in this study and is characterised by a sudden contraction from the calming section diameter to the test section diameter. The test section was manufactured from a 316L stainless steel tube with an inside and outside diameter of 4 mm and 6 mm, respectively. The total length of the stainless steel tube was 6 m, however temperature measurements were only taken across 5.5 m. In order to prevent any upstream effects from influencing the measurements at the last thermocouple station, 0.5 m was allowed between the last thermocouple station (at x = 5.5 m) and the mixer (at x = 6 m). The test section was divided into a developing flow section and a fully developed flow section. The theoretical thermal entrance length ($L_t = 0.05RePrD$) for forced convection laminar flow at a Reynolds number of 2 300 and Prandtl number of 6 was calculated to be 2.4 m. Therefore, the first 2.4 m of the test section was devoted to developing flow, and the remaining tube length to fully developed flow. The total length of the test section provided a maximum length-to-inside diameter ratio (x/D) of 1 373, while previous studies by Ghajar and co-workers [2-4, 6, 7, 9, 10] and Meyer and Olivier [12] had maximum values of approximately 400 and 350, respectively.

The test section was insulated with 120 mm thick insulation with a thermal conductivity of 0.034 W/m.K and the maximum theoretical heat loss was calculated to be 2.6%.

T-type copper-constantan thermocouples were used to measure the surface temperatures at 27 thermocouple stations along the test section, as shown in Figure 2. Four thermocouples were spaced along the circumference, 90° apart, to investigate possible circumferential temperature distributions caused by secondary flow. In the developing section, stations A-R contained four thermocouples each, while stations S-FF in the fully developed section contained three thermocouples each (T1, T3 and alternating T2 and T4). The inlet water temperature was measured using a Pt100 inside the calming section, while the outlet water temperature was measured using a Pt100 inside the mixing section. The purpose of the mixing section was to ensure a uniform outlet temperature and the mixer design was based on the work done by Bakker *et al*. [18].

The thermocouples were glued to the stainless steel tube using Arctic Alumina thermal adhesive which had a thermal conductivity of 9 W/m.K and a curing time of 5 min. As the wall thickness of the stainless steel tube was 1 mm, 0.5 mm indentations were drilled in which the thermocouples were placed. A 3D printed jig was used to ensure that all the indentations were drilled to the same depth. The thermocouples were checked to ensure good contact with the tube. In-situ calibration was done after the test section was built completely.

A constant heat flux boundary condition was obtained by passing current through the tube wall. The 316L stainless steel tube had an electrical resistivity of 74 μΩcm (at 20 °C). As resistivity is a function of temperature, it is expected to increase as the heat flux and tube diameter is increased. The resistance of the stainless steel tube was measured to be 0.282 Ω in the temperature-controlled lab, using a multimeter. The test section

was electrically insulated with Kapton film before it was thermally insulated.

DATA REDUCTION

The mean fluid temperature at the inlet, T_i, and outlet, T_e, of the test section, were measured using Pt100 probes in the calming section and mixing section, respectively. As a constant heat flux boundary condition was applied to the test section, the average axial temperature of the water increased linearly. The mean fluid temperature, T_m, at a specific tube location, x, was obtained using a linear temperature distribution between the inlet and outlet temperatures of the fluid:

$$T_m = \left(\frac{T_o - T_i}{L}\right)x + T_i \tag{1}$$

The bulk fluid temperature, T_b, was the average of the inlet and outlet temperatures of the fluid:

$$T_b = \frac{T_i + T_o}{2} \tag{2}$$

The properties of water (density, ρ, dynamic viscosity, μ, kinematic viscosity, ν, thermal conductivity, k, specific heat, C_p, Prandtl number, Pr, and thermal expansion coefficient, β) were determined using the thermophysical correlations for liquid water [19] at the bulk fluid temperature for the average properties, and at the mean fluid temperature for the local properties at a specific point x, measured from the inlet of the test section.

The Reynolds number was calculated as:

$$Re = \frac{\dot{m}D}{\mu A_c} \tag{3}$$

where $\dot{m}$ was the measured mass flow rate inside the tube, D was the inner-tube diameter, μ was the dynamic viscosity and A_c is the cross-sectional area of the test section.

The cross-sectional area of the test section was calculated as follows:

$$A_c = \frac{\pi}{4}D^2 \tag{4}$$

The electrical energy input ($\dot{Q}_{electric} = VI$) remained constant, resulting in a constant heat flux. The heat transfer rate to the water, $\dot{Q}_w$, was determined from the measured mass flow rate, inlet and outlet temperatures of the fluid and the specific heat capacity which was calculated at the bulk fluid temperature:

$$\dot{Q}_w = \dot{m}C_p(T_o - T_i) \tag{5}$$

The heat transfer rate to the water, $\dot{Q}_w$, was continuously monitored by comparing it to the electrical power, $\dot{Q}_{electric}$, of the power supply, which should ideally be equal since the test section was well insulated. The energy balance, EB, which ideally should be as close as possible to zero, was determined as:

$$EB = \left|\frac{VI - \dot{m}C_p(T_o - T_i)}{VI}\right| * 100 \tag{6}$$

The average energy balance of all the experiments that were conducted was less than 3%, which is in good agreement with the insulation calculations.

The heat flux on the inside of the test section was determined from the heat transfer rate to the water, $\dot{Q}_w$, and the inner surface area, A_s, of the test section along the heated length:

$$\dot{q} = \frac{\dot{Q}_w}{A_s} = \frac{\dot{m}C_p(T_o - T_i)}{\pi DL} \tag{7}$$

The heat transfer rate to the water was used since it was regarded as more accurate than the electrical power input. As the energy balance was not zero, and some losses did occur to the ambient air, the electrical power input was always slightly higher than the heat transfer rate to the water.

The average of the four (or three) temperature measurements at a station was used as the surface temperature at a specific thermocouple station, T_w:

$$T_w = \frac{T_1 + T_2 + \cdots + T_n}{n} \tag{8}$$

The average surface temperature of the test section was calculated from all the temperature measurements on the test section, using the trapezoidal rule:

$$\overline{T}_W = \frac{1}{L}\int_0^L T_w(x)\,dx \tag{9}$$

The thermal resistance across the tube wall was calculated using the following equation:

$$R_{tube} = \frac{ln\left(\frac{D_o}{D}\right)}{2\pi Lk} \tag{10}$$

The thermal conductivity of 316L stainless steel is only 16.3 W/m.K, therefore the temperature difference across the tube wall was calculated using Eq. (11), since the thermal resistance and heat input were known:

$$\Delta T = \dot{Q}_w R_{tube} \tag{11}$$

The thermal resistance was calculated to be 3.63×10^{-4} °C/W. Although the thermocouples were placed in an 0.5 mm deep indentation in the tube wall, temperature difference across the remaining 0.5 mm was approximately 0.2 °C when the maximum heat input (603 W) was applied to the test section. As this is not negligible, the temperature difference calculated using Eq. (11) were thus subtracted from the measured surface

temperatures (Eq. (8)), to obtain the temperature on the inside of the test section.

The heat transfer coefficients, were then determined from the following equations, since the heat flux, $\dot{q}$, surface temperature, T_w, and mean fluid temperature, T_m, were available:

$$h = \frac{\dot{q}}{(T_w - T_m)} \tag{12}$$

The Nusselt numbers were determined from the heat transfer coefficients as follows:

$$Nu = \frac{hD}{k} \tag{13}$$

The heat transfer results were also investigated in terms of the Colburn *j*-factor to account for the variation in the Prandtl number. The Prandtl number is a function of C_p, μ and k. It was found that during experiments, the viscosity changed significantly and the Prandtl number varied between 3 and 7, depending on the conditions and location on the test section. The Colburn *j*-factors were calculated from:

$$j = \frac{Nu}{RePr^{\frac{1}{3}}} \tag{14}$$

The Grashof number, was determined using the following equation:

$$Gr = \frac{g\beta(T_w - T_m)D^3}{\nu^2} \tag{15}$$

where 9.81 m/s^2 were used for gravitational acceleration.

The Rayleigh number is the product of the Grashof number and Prandtl number:

$$Ra = Gr\ Pr \tag{16}$$

In general in this study, the percentage error of a measurement or calculated value (M) was determined as follows:

$$\%error = \frac{\left|M_{measured} - M_{predicted}\right|}{M_{measured}} * 100 \tag{17}$$

The average percentage error was taken as the average of the absolute errors of the data points.

For the purposes of this study, the width of the transitional flow regime was defined as:

$$\Delta Re = Re_{lre} - Re_{cr} \tag{18}$$

UNCERTAINTIES

The method suggested by Dunn [20] was used to calculate the uncertainties of the test section and all the uncertainties were calculated within the 95% confidence interval. The uncertainties of the thermocouples and Pt100's were calculated to be 0.1ºC and 0.031ºC, respectively. The Reynolds number uncertainty remained approximately constant at 1.5% in the laminar and turbulent flow regimes, but increased to 2% in the transitional flow regime due to the fluctuations inside the test section. The Nusselt number and Colburn *j*-factor uncertainties were between approximately 2% and 5% (depending on the heat flux) in the laminar flow regime, but increased as the Reynolds number was increased due to the decreasing temperature difference between the inlet and outlet of the test section, as well as between the surface and fluid. Both Nusselt number and Colburn *j*-factor uncertainties were slightly higher (5-10%) during transition due to the temperature fluctuations which occurred inside the tube.

VALIDATION

For fully developed flow in a circular smooth tube with a constant heat flux boundary condition, the theoretical Nusselt number should be approximately 4.36 [21]. At a Reynolds number of 965 and heat flux of 1 kW/m^2, the average fully developed Nusselt number ($307 \leq x/D \leq 1\ 373$) was found to be 4.5, which was within 3.4% of the theoretical value of 4.36. The local Nusselt numbers were also compared with the correlation of Shah and London [22] and the average deviation was 1.7%. A maximum deviation of 65% was obtained at the inlet, while the deviation was less than 3% between $x/D = 567$ and $x/D = 724$. It could therefore be concluded that secondary flow effects were negligible and that fully developed forced convection measurements were successfully obtained in the laminar flow regime.

The average laminar Nusselt numbers obtained at Reynolds numbers between 100 and 2 000 using a heat flux of 3 kW/m^2, were used to validate the average laminar Nusselt numbers for mixed convection conditions. Ghajar and Tam [2] considered the flow to be dominated by mixed convection when the Nusselt numbers deviated more than 15% from the corresponding forced convection Nusselt numbers. This was regarded as a conservative approach since Metais and Eckert [23] used a deviation of 10%. The average laminar Nusselt numbers varied between 5.3 and 5.6, which was more than 20% greater than the fully developed forced convection Nusselt number of 4.36, which confirmed that the flow was dominated by mixed convection. The results correlated well with the correlation of Morcos and Bergles [24] and the average deviation was 4%.

To validate the turbulent Nusselt numbers, the Reynolds number was varied between 4 600 and 8 000 and a heat flux of 8 kW/m^2 was applied. The turbulent Nusselt numbers correlated very well with the equation of Gnielinski [25] and the average deviation was less than 1%. The results also correlated well with the correlation of Ghajar and Tam [4] with an average deviation of 3.2%.

RESULTS

The Reynolds number, Nusselt number and Colburn *j*-factors were calculated at each thermocouple station (Figure 2) and compared with each other. The results presented in Figures 3 and 4 therefore represents the local heat transfer results, calculated using the properties evaluated at the local temperatures. A total of 176 tests were conducted which consisted of 176 mass flow rate measurements and 19 008 temperature measurements.

Forced Convection

Figure 3 contains the Colburn *j*-factors as a function of Reynolds number at a heat flux of 1 kW/m^2 for *x/D* = 22 to *x/D* = 349 (Figure 3(a)) and *x/D* = 392 to *x/D* = 1 311 (Figure 3(b)). The Reynolds number was varied between 900 and 6 000 to ensure that the whole transitional flow regime, as well as sufficient parts of the laminar and low-Reynolds-number-end flow regimes, was covered. It was not feasible to increase the Reynolds number above 6 000 to the fully turbulent flow regime, since the uncertainty of the heat transfer coefficients became too large due to the small temperature differences inside the test section.

The flow was laminar between Reynolds numbers of 900 and approximately 2 000 (depending on the tube location), since the Colburn *j*-factors formed a straight diagonal line. From Figure 3(a) it follows that the laminar Colburn *j*-factors were a maximum at the inlet of the test section and then decreased, as the flow developed and approached fully developed flow. Furthermore, the gradient of the laminar Colburn *j*-factors increased as *x/D* increased. This is due to the developing thermal boundary layer. At a fixed Reynolds number of 2 000, the flow was closer to fully developed at *x/D* = 349 than at *x/D* = 22, which explains why the Colburn *j*-factors at *x/D* = 22, were greater than at *x/D* = 349. Furthermore, the thermal entrance length increased with increasing Reynolds number. At a fixed thermocouple station of *x/D* = 22, the flow was closer to fully developed flow as the Reynolds number was decreased. The difference between the laminar Colburn *j*-factors of the different Reynolds numbers became negligible after *x/D* = 305. Although the flow was not yet fully developed, the change in thermal boundary layer thickness with axial position became negligible between the stations.

From Figure 3(a) it also follows that at *x/D* = 22 transition started (Re_{cr}) at a Reynolds number of 1 900, while it started at a Reynolds number of 1 950 at *x/D* = 349. Although it seems as if transition was slightly delayed along the test section, this was not the case. Transition started at the same moment in time along the entire test section and the increasing Reynolds number was only due to the variation in the fluid properties. As a constant heat flux was applied, the fluid temperature increased along the test section, thus the local fluid properties varied which caused the local Reynolds numbers to vary (increase). However, as this was for forced convection conditions and only a small heat flux was applied, the temperature difference and thus Reynolds number difference was small. Furthermore, the gradient of the Colburn *j*-factors in the transitional flow regime increased slightly with axial position. Although it was challenging to identify the end of the transitional flow regime (Re_{lre}) point near the inlet of the test section, it became more pronounced as the flow developed along the tube length.

From the Colburn *j*-factors in Figure 3(a) it also follows that transition ended earlier as the flow developed along the test section, therefore the width of the transitional flow regime (ΔRe) decreased. In the transitional flow regime, the boundary layer was laminar when the flow entered the tube, but then passed through a transition region before it became turbulent. As the Reynolds number was increased, the increased velocity of the fluid caused the flow to transition to turbulent faster, therefore the transition region in terms of axial position decreased and a larger portion of the test section contained turbulent flow. This implies that at two fixed axial positions (for example *x/D* = 22 and *x/D* = 349), *x/D* = 22 will experience transition for a wider Reynold number range than *x/D* = 349, which explains why the width of the transitional flow regime decreased along the tube length.

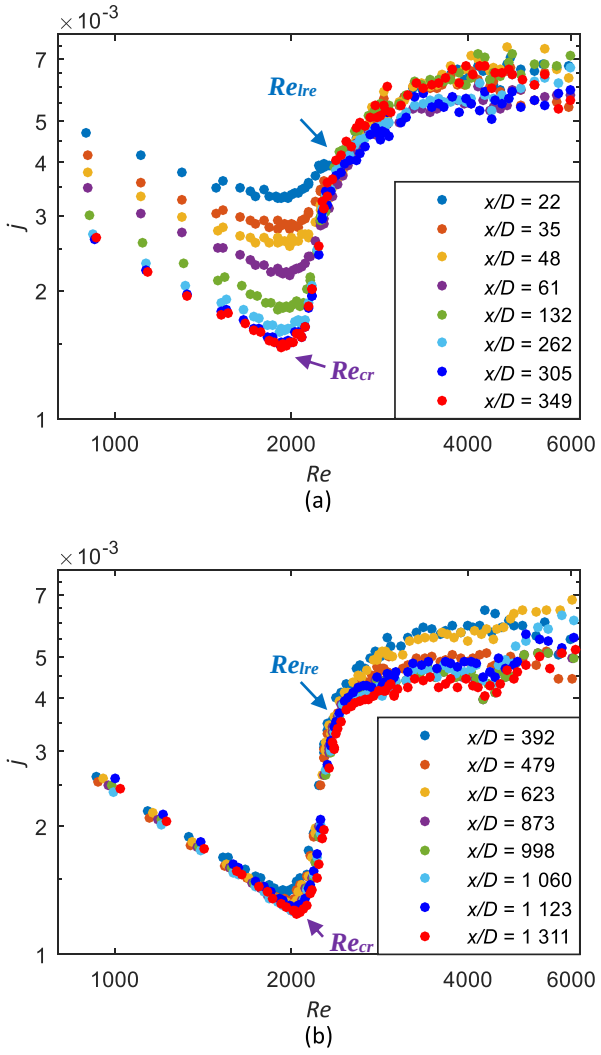

Figure 3 Comparison of local Colburn *j*-factors as a function of Reynolds number at a heat flux of 1 kW/m^2 for (a) *x/D* = 22 to *x/D* = 349 and (b) *x/D* = 392 to *x/D* = 1 311

Furthermore, from Figure 3(a) it follows that the position of the thermocouple station along the test section had no significant influence on the trend of the heat transfer coefficients in the low-Reynolds-number-end regime, since the shape of the Colburn *j*-factors remained approximately the same. No significant changes along the tube length were expected in thus regime since the flow was almost fully turbulent (and thus fully developed). Although the magnitude of the heat transfer coefficients between the thermocouple stations varied in this regime, this was due to the increased uncertainties of the temperature measurements. The temperature differences were significantly smaller than in the laminar and transitional flow regimes, which led to higher Colburn *j*-factor uncertainties. If one thermocouple station measured a slightly higher temperature (although it was still within the uncertainty of the thermocouple), the Colburn *j*-factors at that thermocouple was also higher compared to the rest.

Figure 3(b) contains the Colburn *j*-factors in the remaining part ($392 \leq x/D \leq 1\,311$) of the test section. As the flow was either very close to fully developed or fully developed, there was no significant difference between the heat transfer coefficients of the different thermocouple stations in the laminar flow regime. From the Colburn *j*-factors in Figure 3(b) it follows that transition was once again slightly delayed along the test section due to the variation of the fluid properties with temperature. The transition gradient increased slightly between $x/D = 392$ and $x/D = 623$, but remained approximately constant further along the test section. Between $x/D = 392$ and $x/D = 623$, transition ended slightly earlier with axial position, causing the width of the transitional flow regime to decrease. However, beyond $x/D = 623$, the width of the transitional flow regime remained constant, therefore the transition gradient remained approximately constant.

Mixed Convection

The Colburn *j*-factors at $x/D = 22$ to $x/D = 1\,373$ are compared at a heat flux of 3 kW/m^2 in Figure 4(a) and at a heat flux of 8 kW/m^2 in Figure 4(b). The Reynolds number was varied between 800 and 8 000 to ensure that the whole transitional and low-Reynolds-number-end flow regimes, as well as sufficient parts of the laminar and turbulent flow regimes, were covered. Although the bulk Reynolds number was not decreased below 1 800 at a heat flux of 8 kW/m^2 (the outlet temperature exceeded 70 °C), a sufficient part of the laminar flow regime was still covered. Furthermore, the Reynolds number was not increased beyond 8 000 since the temperature differences became too small and the uncertainties too high to obtain accurate and reliable results.

When comparing the laminar Colburn *j*-factors of the two heat fluxes, it follows that between $x/D = 22$ and $x/D = 61$, there was no significant difference in the trend and magnitude of the Colburn *j*-factors of the two heat fluxes. However, as x/D was increased further, the gradient of the laminar Colburn *j*-factors did not only increase along the test section, but also with increasing heat flux. This is due to the combined effects of developing flow and free convection effects. Between $x/D = 22$ and $x/D = 61$, the thermal boundary layer thickness was not sufficient for free convection effects to become significant. However, as x/D was increased further, the thermal boundary layer thickness increased and free convection effects became significant. The gradients of the laminar Colburn *j*-factors increased with axial position between $x/D = 132$ and $x/D = 349$ and increased further as the heat flux was increased. As the Reynolds number was decreased from 2 000 to 1 000, the thermal entrance length decreased. Therefore, at a fixed axial position, the thermal boundary layer thickness (and thus free convection effects) increased. This led to increased heat transfer coefficients, which explains why the gradient of the Colburn *j*-factors increased with increasing x/D.

From Figure 4, it also follows that free convection effects (due to the increased heat flux) caused transition to occur earlier between $x/D = 22$ and $x/D = 61$, while it was delayed as x/D was increased further. Similar to the forced convection results, transition occurred at the same moment along the entire test section and the increasing Reynolds numbers were only due to the variation of the fluid properties along the test section. At a heat flux of 3 kW/m^2, transition occurred at a mass flow rate of 0.00573 kg/s, while it occurred at 0.00556 kg/s when the heat flux was increased to 8 kW/m^2. Therefore, although it seemed as if transition was delayed, free convection effects actually caused transition to occur earlier. The increased free convection effects led to increased temperature fluctuations inside the test section, which caused the flow to become unstable at lower mass flow rates. Although transition occurred earlier (lower mass flow rates) with increasing heat flux, the bulk critical Reynolds number increased, since the surface temperatures (and variation of the fluid properties) along the tube length increased significantly. This increased temperature gradient along the test section caused the critical Reynolds numbers of the difference heat fluxes to cross at approximately $x/D = 95.7$, and to increase with increasing heat flux as x/D was increased further.

Similar to Figure 3, the transition gradient increased with x/D as the flow approached fully developed flow and became approximately constant after $x/D = 998$. However, the gradient of the Colburn *j*-factors in the transitional flow regime also increased as the heat flux was increased. Therefore, free convection effects caused the flow to transition faster from laminar to turbulent along the tube length. This explains why at a fixed axial position, the transition gradient increased and the width of the transitional flow regime increased.

From Figure 4 it also follows that free convection effects did not have a significant influence on the end of the transitional flow regime between $x/D = 22$ and $x/D = 349$ and the width of the transitional flow regime remained approximately constant. However, the heat transfer coefficients in the low-Reynolds-number-end flow regime increased with increasing heat flux and thus free convection effects. Furthermore, when comparing Figure 4(a) and (b) it follows that the width of the low-Reynolds-number-end regime decreased with increasing heat flux. The flow is said to be fully turbulent once the Colburn *j*-factors formed a straight diagonal line (as indicated by the black dotted line in Figure 4). As expected, there was no significant difference between the turbulent heat transfer coefficients of the different heat fluxes, since the free convection effects were

suppressed by the fluid motion. The scatter in heat transfer coefficients in the low-Reynolds-number-end and turbulent flow regimes also decreased with increasing heat flux, due to the increased temperatures that led to decreased uncertainties.

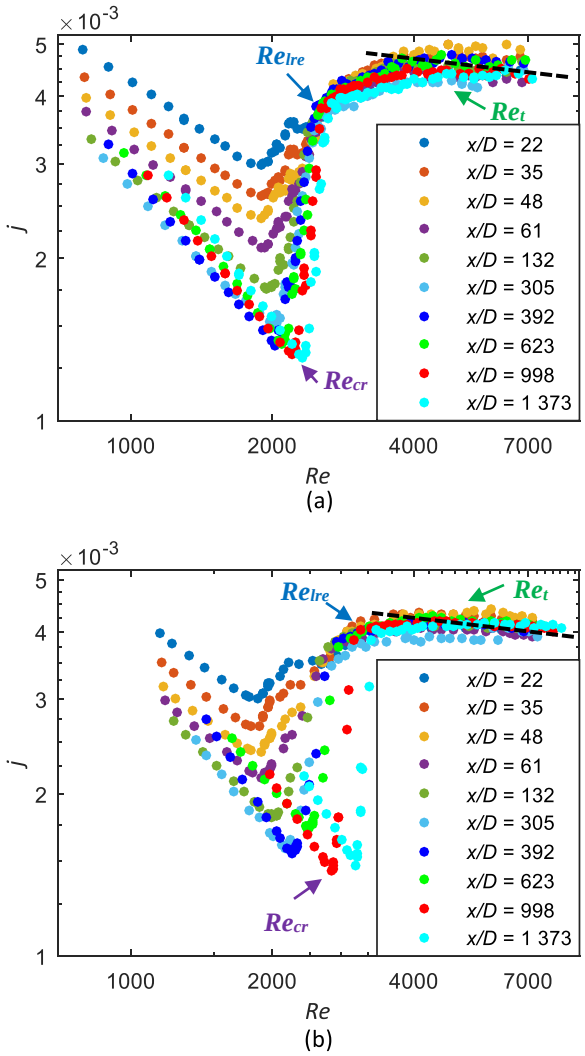

Figure 4 Comparison of local Colburn *j*-factors as a function of Reynolds number for *x/D* = 22 to *x/D* = 1 373 at a heat flux of (a) 3 kW/m^2 and (b) 8 kW/m^2

Transition region

To gain a better understanding on how the transition region varies as the flow develops along the test section, as well as the influence of free convection effects, the Reynolds numbers at which transition started (Re_{cr}) and ended (Re_{lre}) are summarised in Figure 5(a), while Figure 5(b) compares the width of the transition flow regime (ΔRe) for the different heat fluxes. The empty markers in Figure 5(a) represent the start of the transitional flow regime, while the filled markers represent the end of the transitional flow regime. Although it seems from Figure 5(a) as if transition was delayed along the test section, this was not the case. As concluded from Figure 4, the increasing Reynolds numbers were only due to the increasing temperatures along the test section, and free convection effect actually caused transition to occur earlier. Furthermore, the gradient of Re_{cr}-line increased with increasing heat flux, since the temperature gradient along the test section increased.

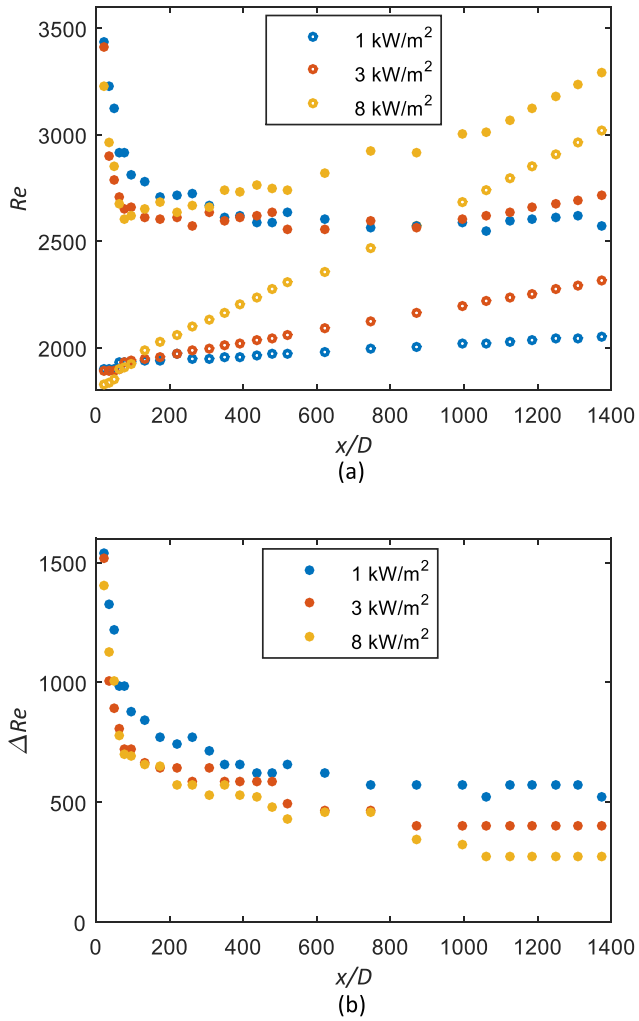

Figure 5 Comparison of (a) Reynolds numbers at which transition started and ended and (b) width of transition region, as a function of axial position at a heat fluxes of 1, 3 and 8 kW/m^2

From Figure 5(a) it follows that the end of the transitional flow regime occurred earlier with increased axial position near the inlet of the test section, but was then delayed as *x/D* was increased further. However, from Figure 5(b) it follows that the width of the transition region decreased as the flow developed and then became approximately constant. Since transition started at the same moment along the entire test section, and it follows from Figure 5(b) that the width of the transitional flow regime decreased along the test section, it can be concluded that the end of transition occurred earlier along the test section as the flow developed. The increased Reynolds numbers were thus once again due to the variation of fluid properties with temperature. Furthermore, the width of the transition region also decreased as the heat flux was increased. The minimum width of the transitional flow regime was a Reynolds number

range of 580 at a heat flux of 1 kW/m^2, but it decreased to 270 when the heat flux was increased to 8 kW/m^2. This confirms that free convection effects, caused the flow to transition faster from laminar to turbulent, therefore the transition region inside the test section decreased as well as the Reynolds number range of the transitional flow regime.

From Figure 5(b) it also follows that when free convection effects were negligible and forced convections existed (1 kW/m^2), the width of the transitional flow regime gradually decreased as the flow developed. After x/D = 748, the width of the transitional flow regime became constant at a Reynolds number range of 570. An interesting observation is that, as the heat flux was increased and free convection effects increased, the axial position at which the width of the transitional flow regime became constant increased, implying that a longer length was required for the flow to transition from laminar to turbulent. It therefore seems as if free convection effects disrupted the stability of the thermal boundary layer, leading to longer required tube length for the flow to become fully turbulent.

CONCLUSION

Up to now, no experimental work has been done specifically focussing on how free convection effects influence the local heat transfer characteristics in the transitional flow regime. The purpose of this study was therefore to experimentally investigate the influence of free convection on the local heat transfer characteristics of developing and fully developed flow in smooth tubes in the transitional flow regime. The Reynolds number was varied between 900 and 8 000 to ensure that the whole transitional and low-Reynolds-number-end regimes, as well as sufficient parts of the laminar and turbulent flow regimes, were covered.

The local Colburn *j*-factors were calculated at each of the 27 thermocouple stations and then compared with each other for both forced and mixed convection conditions. The start of transition was not influenced by the characteristics of developing flow and occurred at the same time along the whole tube length during both forced and mixed convection conditions. Although free convection effects caused transition to occur earlier (at a lower mass flow rate), the critical Reynolds number increased due to the increased temperatures, and variation of the fluid properties, along the test section. The end of transition was influenced by the development of the thermal boundary layer as well as free convection effects. As transition ended earlier as the flow developed along the test section, as well as with increasing free convection effects, the width of the transitional flow regime decreased. It can therefore be concluded that the heat transfer characteristics of developing and fully flow in the transitional flow regime are significantly different and free convection effects caused the flow to transition faster from laminar to turbulent along the test section, therefore the Reynolds number range of the transitional flow regime decreased.

ACKNOWLEDGEMENTS

The funding obtained from the NRF, Stellenbosch University/ University of Pretoria Solar Hub, CSIR, EEDSM Hub, RDP and NAC is acknowledged and duly appreciated.

REFERENCES

[1] J. P. Meyer, "Heat transfer in tubes in the transitional flow regime," presented at the 15th International Heat Transfer Conference, Kyoto, Japan, 2014.

[2] A. J. Ghajar and L. M. Tam, "Laminar-transition-turbulent forced and mixed convective heat transfer correlations for pipe flows with different inlet configurations," in *Winter Annual Meeting of the American Society of Mechanical Engineers*, New York, United States, 1991, pp. 15-23.

[3] A. J. Ghajar and K. F. Madon, "Pressure drop measurements in the transition region for a circular tube with three different inlet configurations," *Experimental Thermal and Fluid Science*, vol. 5, pp. 129-135, 1992.

[4] A. J. Ghajar and L. M. Tam, "Heat transfer measurements and correlations in the transition region for a circular tube with three different inlet configurations," *Experimental Thermal and Fluid Science*, vol. 8, pp. 79-90, 1994.

[5] A. J. Ghajar and L. M. Tam, "Flow regime map for a horizontal pipe with uniform wall heat flux and three inlet configurations," *Experimental Thermal and Fluid Science*, vol. 10, pp. 287-297, 1995.

[6] L. M. Tam and A. J. Ghajar, "Effect of Inlet Geometry and Heating on the Fully Developed Friction Factor in the Transition Region of a Horizontal Tube," *Experimental Thermal and Fluid Science*, vol. 15, pp. 52-64, 1997.

[7] L. M. Tam and A. J. Ghajar, "The unusual behavior of local heat transfer coefficient in a circular tube with a bell-mouth inlet," *Experimental Thermal and Fluid Science*, vol. 16, pp. 187-194, 1998.

[8] A. J. Ghajar, C. C. Tang, and W. L. Cook, "Experimental investigation of friction factor in the transition region for water flow in minitubes and microtubes," *Heat Transfer Engineering*, vol. 31, pp. 646-657, 2010.

[9] H. K. Tam, L. M. Tam, A. J. Ghajar, S. C. Tam, and T. Zhang, "Experimental investigation of heat transfer, friction factor, and optimal fin geometries for the internally microfin tubes in the transition and turbulent regions," *Journal of Enhanced Heat Transfer*, vol. 19, pp. 457-476, 2012.

[10] H. K. Tam, L. M. Tam, and A. J. Ghajar, "Effect of inlet geometries and heating on the entrance and fully-developed friction factors in the laminar and transition regions of a horizontal tube," *Experimental Thermal and Fluid Science*, vol. 44, pp. 680-696, 2013.

[11] L. M. Tam, H. K. Tam, A. J. Ghajar, W. S. Ng, and C. K. Wu, "The effect of inner surface roughness and heating on friction factor in horizontal mini-tubes," presented at the 15th International Heat Transfer Conference, Kyoto, Japan, 2014.

[12] J. A. Olivier and J. P. Meyer, "Single-phase heat transfer and pressure drop of the cooling of water inside smooth tubes for transitional flow with different inlet geometries (RP-1280)," *HVAC and R Research*, vol. 16, pp. 471-496, 2010.

[13] J. P. Meyer and J. A. Olivier, "Transitional flow inside enhanced tubes for fully developed and developing flow with different types of inlet disturbances: Part II-heat transfer," *International Journal of Heat and Mass Transfer*, vol. 54, pp. 1598-1607, 2011.

[14] J. P. Meyer and J. A. Olivier, "Transitional flow inside enhanced tubes for fully developed and developing flow

with different types of inlet disturbances: Part I - Adiabatic pressure drops," *International Journal of Heat and Mass Transfer*, vol. 54, pp. 1587-1597, 2011.

[15] J. P. Meyer and J. A. Olivier, "Heat transfer and pressure drop characteristics of smooth horizontal tubes in the transitional flow regime," *Heat Transfer Engineering*, vol. 35, pp. 1246-1253, 2014.

[16] L. M. Tam, A. J. Ghajar, H. K. Tam, and S. C. Tam, "Development of a flow regime map for a horizontal pipe with the multi-classification Support Vector Machines," in *2008 Proceedings of the ASME Summer Heat Transfer Conference, HT 2008*, 2009, pp. 537-547.

[17] H. K. Tam, L. M. Tam, A. J. Ghajar, and C. W. Cheong, "Development of a unified flow regime map for a horizontal pipe with the support vector machines," in *AIP Conference Proceedings*, 2010, pp. 608-613.

[18] A. Bakker, R. D. LaRoche, and E. M. Marshall. (2000, 24 February). *Laminar flow in static mixers with helical elements*. Available: http://www.bakker.org/cfmbook/lamstat.pdf

[19] C. O. Popiel and J. Wojtkowiak, "Simple formulas for thermophysical properties of liquid water for heat transfer calculations [from O°C to 150°C," *Heat Transfer Engineering*, vol. 19, pp. 87-101, 1998.

[20] P. F. Dunn, *Measurement and Data Analysis for Engineering and Science*, 2nd ed. United States of America: CRC Press, 2010.

[21] Y. A. Cengel, *Heat and Mass Transfer: A Practical Approach*, 3rd ed. Singapore: McGraw-Hill, 2006.

[22] R. K. Shah and A. L. London, *Laminar Flow Forced Convection in Ducts*. New York: Academic Press, 1978.

[23] B. Metais and E. Eckert, "Forced, mixed, and free convection regimes," *Journal of Heat Transfer*, vol. 86, pp. 295-296, 1964.

[24] S. M. Morcos and A. E. Bergles, "Experimental investigation of combines forced and free laminar convection in horizontal tubes," *Journal of Heat Transfer*, vol. 97, pp. 212-219, 1975.

[25] V. Gnielinski, "New equations for heat and mass-transfer in turbulent pipe and channel flow," *International Chemical Engineering*, vol. 16, pp. 359-368, 1976.